JOURNAL OF COMPUTATIONAL PHYSICS 78, 231–248 (1988)

Incompressible Flow in Porous Media with Two Moving Boundaries

PAUL PAPATZACOS AND SVEN-ÅKE GUSTAFSON

Rogaland University, Stavanger, Norway.

Received November 13, 1985; revised September 9, 1987

The industrial process considered is production of oil through a horizontal well perforated into an oil-zone which is bounded below by water and bounded above by gas. This process is modelled by a two-dimensional, incompressible, porous-medium flow into a point sink. The interfluid boundaries are then moving boundaries. The conditions at each moving boundary are expressed, with appropriate assumptions, as equations between the fluid potential and the vertical displacement of the boundary. There is one static and one dynamic condition at each boundary. Boundary-fitted orthogonal coordinates are then introduced. The Laplace equation for the vertical displacement and the Poisson equation for the velocity potential, together with the static boundary conditions, can then be solved analytically, in terms of the vertical displacement at each boundary, with time as a parameter. The vertical displacement at each boundary must be calculated at each time-step by solving the equations expressing the dynamic boundary conditions. These are coupled, non-linear integro-differential equations. The solution is expressed as an infinite trigonometric series, whose coefficients are determined as the solution of an infinite system of ordinary differential equations. Convergence acceleration is applied to this series and hence only the first few terms need to be calculated.

1. INTRODUCTION

The problem considered in this paper has its background in the petroleum industry, specifically in the exploitation of thin but areally extensive oil-zones sandwiched between a water-zone at the bottom and a gas-zone at the top. Because of the small thickness of the oil-zone it is advantageous to bore a long well horizontally into the porous medium of the oil-zone.

The production of oil in such a configuration raises a number of questions, the most important ones being the following. First, what is the time (called critical time) at which one or both of the adjacent fluids break through at the well. Second, how to position the well-axis in the oil zone so that the critical time is maximum, for a given rate of production and given fluid properties. And third, how does pressure in the immediate vicinity of the well vary with time. Knowledge of a theoretical pressure versus time curve leads, by comparison with the measured pressure and with the use of reservoir engineering methods, to the determination of reservoir properties.

0021-9991/88 $3.00

The model which has been set up to answer these question is now briefly described. In a vertical plane V, perpendicular to the axis of the well and away from its ends, one has the two-dimensional flow of three immiscible fluids, identified as g (gas), o (oil), and w (water), with intrinsic masses ρ satisfying

$$\rho_g < \rho_0 < \rho_w.$$

Neglecting forces due to capillary pressure, the three liquids are at all times separated by well-defined surfaces intersecting V along two lines as shown in Fig. 1. Assuming that the well has zero radius, its intersection with V is a point. One then obtains in V two-dimensional flow with a point sink and two moving boundaries (Fig. 1). Both boundaries move inwards when fluid o is drawn into the sink and one has a phenomenon analogous to "coning" [1], also called the "Muskat problem" [2]. It is expected that, as shown by Muskat [1], an unstable situation will occur before any of the boundaries has reached the sink. It has been shown in calculations of related problems [3–5] that one should expect a breakdown of the solution to occur at a time (the critical time) when a cusp appears at a boundary.

Further assumptions will be introduced in the next section, so that the model which is set up concentrates on the description of flow for fluid o as a two-dimensional moving boundary problem. Similar problems, arising in particular in Hele–Shaw flow [3, 6] have been solved by conformal mapping. This consists in mapping the physical flow into the complex plane in such a way that the moving boundary is mapped onto the unit circle, so that the complex potential (the real part of which is the pressure) becomes easy to find in the mapped plane. The pressure for the physical flow is then obtained in terms of the mapping function

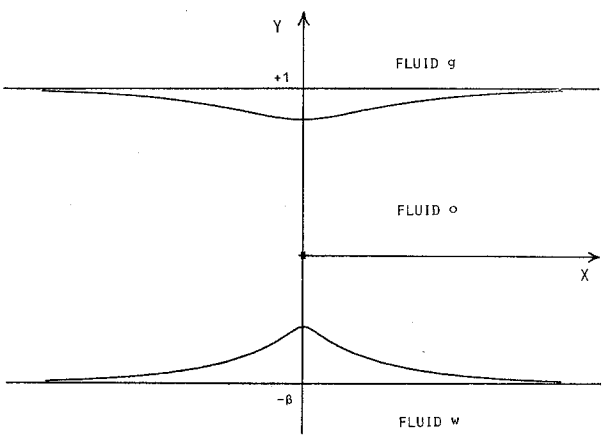

FIG. 1. The x-axis is horizontal, the y-axis vertical. The well is horizontal, with axis perpendicular to the x–y plane and cutting the x–y plane at the origin. The fluids are originally separated by two parallel planes and, later, by curved surfaces. Note that the distance between well-axis and upper initial interface is the unit of length.

which is itself calculated by using complex variable theory [3–6]. The applicability of the method just outlined depends on the pressure having at all times a constant value on the moving boundary. A theorem in complex analysis [7] then guarantees that the complex potential in the mapped plane has that same constant value on the unit circle. If the pressure is not constant on the moving boundary then the complex potential on the unit circle of the mapped plane depends on the mapping function and the methods established for Hele–Shaw flow are then not directly applicable.

The model which is presented in the next section is such that the pressure at the moving boundaries depends on the displacement of the boundaries so that flow is not of the Hele–Shaw type. The method which is presented for solving this moving-boundary problem is based on the use of boundary-fitted orthogonal coordinates [8]. It will be shown that the moving-boundary problem is transformed into two classical boundary value problems (one for the pressure and one to determine the new coordinates) and one initial value problem. The two boundary value problems admit closed-form solutions in terms of the vertical displacements of the boundaries, which are in turn determined by the solution to the initial value problem. As will be shown, this initial value problem is formulated as a system of two non-linear integro-differential equations. Its solution will be given by two methods, one of which, to our knowledge, has not been previously presented. It consists of a first step whereby the two integro-differential equations are transformed into an infinite set of ordinary, first-order differential equations [9] and of a second step which solves the question of closure by using acceleration of convergence. This method is valid for small rates of fluid withdrawal. The other method of solution uses iteration and is valid for large rates. The regions of validity overlap so that one is able to answer the questions at the beginning of this section.

2. The Model: Flow Equation and Boundary Conditions

2.1. *Main Assumptions*

The equation describing flow in a porous medium is a diffusion equation for the velocity potential ϕ, with a right-hand side accounting for possible sources or sinks. It will be assumed that compressibility is zero so that the time-derivative drops out and one obtains, for fluid o,

$$(\partial^2/\partial x^2 + \partial^2/\partial y^2)\,\phi = 2\pi Q\,\delta(x)\,\delta(y), \tag{1}$$

where $\delta(x)$ is Dirac's delta-function and Q is the constant rate of withdrawal by the sink. Note that the sink is placed at the origin of the coordinate axes (Fig. 1) and that the distance from the sink to the initial upper interface is taken as the unit of length. The distance from the sink to the initial lower interface is denoted by β. All quantities in (1) are dimensionless. Formulas relating dimensionless and physical quantities are given in the Appendix.

An essential assumption is now introduced concerning fluids g and w, namely that they are, at each time, in static equilibrium. In other words they participate in the movement of the interface boundaries by expanding when pressure falls, but their flow is neglected. The approximation implied by this assumption is expected to be good because fluid velocities in porous media are usually very low at a distance from sources and sinks. We shall return to this implication later on.

The boundary conditions on ϕ are of two types: static and dynamic.

2.2. *Static Boundary Conditions*

This set of boundary conditions expresses that the pressure of fluid o is equal to the static pressure in fluid g at the upper boundary and to the static pressure in fluid w at the lower boundary. If (x_U, y_U) and (x_L, y_L) are two points, at the upper and lower boundary, respectively, then it is implied by hydrostatics that

$$\phi(x_L, y_L) = -\psi(y_L + \beta), \tag{2}$$

$$\phi(x_U, y_U) = y_U - 1, \tag{3}$$

where

$$\psi = \frac{\rho_w - \rho_o}{\rho_o - \rho_g}. \tag{4}$$

2.3. *Dynamic Boundary Conditions*

This second set of boundary conditions expresses the velocity of the fluid at a point of a boundary in terms of the velocity potential at that point. These conditions contribute to the definition of the boundary-fitted orthogonal coordinates to be introduced in Section 3, so that we transfer their mathematical formulation to that section.

3. Boundary-Fitted Normal Coordinates

It will now be shown that the moving-boundary problem described above, can be reformulated as a classical boundary value problem by the introduction of boundary-fitted normal coordinates, as described by Ryskin and Leal [8].

Consider a new set of coordinates, (ξ, η). The $\xi = \xi_0$ curves with parametric equations $x = x(\xi_0, \eta)$, $y = y(\xi_0, \eta)$, and the $\eta = \eta_0$ curves with parametric equations $x = x(\xi, \eta_0)$, $y = y(\xi, \eta_0)$ are orthogonal if the functions $x(\xi, \eta)$, $y(\xi, \eta)$ satisfy

$$f\frac{\partial x}{\partial \xi} = \frac{\partial y}{\partial \eta}, \qquad \frac{\partial x}{\partial \eta} = -f\frac{\partial y}{\partial \xi}, \tag{5}$$

where f is an arbitrary distortion function which can be chosen to coincide with that of a known separable coordinate system [8] when analytical calculations are

wished for. We shall here make the choice $f=1$ implying that the new coordintes are of Cartesian type. Furthermore, it is convenient to introduce two functions, $X(\xi, \eta, t)$, and $Y(\xi, \eta, t)$, through

$$x(\xi, \eta, t)=\xi+X(\xi, \eta, t), \tag{6}$$

$$y(\xi, \eta, t)=\eta+Y(\xi, \eta, t). \tag{7}$$

Having chosen $f=1$, these functions satisfy

$$\frac{\partial X}{\partial \xi}=\frac{\partial Y}{\partial \eta}, \qquad \frac{\partial X}{\partial \eta}=-\frac{\partial Y}{\partial \xi}. \tag{8}$$

An equivalent equation for Y, say, is

$$(\partial^2/\partial \xi^2+\partial^2/\partial \eta^2)\, Y=0. \tag{9}$$

Such an equation can also be written for X but, if Y is calculated by solving (9) with appropriate boundary conditions, then X is determined through Eqs. (8).

Since ξ and η are of Cartesian type we set their ranges as

$$-\infty<\xi<+\infty \tag{10}$$

$$-\beta \leqslant \eta \leqslant +1. \tag{11}$$

The lines $\xi=\xi_0 \to +\infty$ $(-\infty)$ are infinitely far to the right (left), and the obvious flow symmetry implies that $\xi=0$ will always represent the y-axis. The line $\eta=-\beta$ $(+1)$ is the lower (upper) boundary. A slight complication arises here with the coordinates (ξ_S, η_S) of the sink. We know that $\xi_S=0$ because of the symmetry but η_S is unknown. As we shall see later, it is a function of time and must be determined as such.

It is then found by direct calculation that (1), (2), and (3) become

$$(\partial^2/\partial \xi^2+\partial^2/\partial \eta^2)\, \phi=2\pi Q\, \delta(\xi)\, \delta(\eta-\eta_S), \tag{12}$$

$$\phi(\xi, -\beta, t)=-\psi Y_w(\xi, t), \tag{13}$$

$$\phi(\xi, 1, t)=Y_g(\xi, t), \tag{14}$$

where, for simplicity, the following notation has been introduced:

$$Y(\xi, -\beta, t)=Y_w(\xi, t), \tag{15}$$

$$Y(\xi, +1, t)=Y_g(\xi, t). \tag{16}$$

We now turn to the formulation of the dynamic boundary conditions (see Section 2.3). A point at a boundary is defined by (ξ_B, η_B), where ξ_B is arbitrary

but fixed while $\eta_B = 1$ (upper boundary) or $-\beta$ (lower boundary). The velocity components of such a point are then, by definition of the velocity potential,

$$\frac{\partial}{\partial t} x(\xi_B, \eta_B, t) = -\left[\frac{\partial \phi}{\partial x}\right]_{\xi_B, \eta_B},$$

$$\frac{\partial}{\partial t} y(\xi_B, \eta_B, t) = -\left[\frac{\partial \phi}{\partial y}\right]_{\xi_B, \eta_B}.$$

The right-hand sides can be expressed in terms of partial derivatives with respect to ξ and η by solving the system of equations:

$$\frac{\partial \phi}{\partial \xi} = \frac{\partial \phi}{\partial x}\frac{\partial x}{\partial \xi} + \frac{\partial \phi}{\partial y}\frac{\partial y}{\partial \xi},$$

$$\frac{\partial \phi}{\partial \eta} = \frac{\partial \phi}{\partial x}\frac{\partial x}{\partial \eta} + \frac{\partial \phi}{\partial y}\frac{\partial y}{\partial \eta}.$$

Using (6)–(8), (15), and (16) one then obtains

$$\frac{\partial Y_w}{\partial t} = \frac{\psi\left[\frac{\partial Y_w}{\partial \xi}\right]^2 - \left[\frac{\partial \phi}{\partial \eta}\right]_{\eta=-\beta}\left[1 + \left[\frac{\partial Y}{\partial \eta}\right]_{\eta=-\beta}\right]}{\left[\frac{\partial Y_w}{\partial \xi}\right]^2 + \left[1 + \left[\frac{\partial Y}{\partial \eta}\right]_{\eta=-\beta}\right]^2}, \tag{17}$$

$$\frac{\partial Y_g}{\partial t} = -\frac{\left[\frac{\partial Y_g}{\partial \xi}\right]^2 + \left[\frac{\partial \phi}{\partial \eta}\right]_{\eta=+1}\left[1 + \left[\frac{\partial Y}{\partial \eta}\right]_{\eta=+1}\right]}{\left[\frac{\partial Y_g}{\partial \xi}\right]^2 + \left[1 + \left[\frac{\partial Y}{\partial \eta}\right]_{\eta=+1}\right]^2}. \tag{18}$$

Similar equations can be written for the X-function but such equations are not needed since X is determined through Y by Eqs. (8). The condition of no displacement at zero time yields

$$Y_w(\xi, 0) = 0, \qquad Y_g(\xi, 0) = 0. \tag{19}$$

Thus the moving-boundary problem presented in Section 2 is transformed into classical boundary value problems for Y and ϕ, and into an initial-value problem for Y_w and Y_g. Using Green functions to solve the boundary-value problem defined by (9), (15), (16), and

$$Y(+\infty, \eta, t) = Y(-\infty, \eta, t) = 0, \tag{20}$$

and using the boundary-value problem defined by (12)–(14) and

$$\phi(+\infty, \eta, t) = \phi(-\infty, \eta, t) = 0, \tag{21}$$

one obtains ϕ and Y as integral transforms of Y_w and Y_g. The initial value problem for Y_w and Y_g defined by (17)–(19) is in the form of two coupled non-linear integrodifferential equations which must be solved numerically.

4. Solutions for the Boundary-Value Problems

The two boundary-value problems defined above can be solved with the same Green function. The latter can be found in Williams [10], written as a Fourier series. Its sum is easily found to be

$$G = \frac{1}{4\pi} \ln \frac{\cosh[C(\xi' - \xi)] - \cos[C(\eta' - \eta)]}{\cosh[C(\xi' - \xi)] - \cos[C(\eta' + \eta + 2\beta)]}, \tag{22}$$

where

$$C = \pi/(1 + \beta). \tag{23}$$

The solutions are then

$$Y(\xi, \eta, t) = U_w(\xi, \eta, t) + U_g(\xi, \eta, t), \tag{24}$$

$$\phi(\xi, \eta, t) = -\psi U_w(\xi, \eta, t) + U_g(\xi, \eta, t) + \frac{Q}{2} \ln \frac{\cosh(C\xi) - \cos[C(\eta_S - \eta)]}{\cosh(C\xi) - \cos[C(\eta_S + \eta + 2\beta)]}, \tag{25}$$

where

$$U_w = \frac{C}{2\pi} \int_{-\infty}^{+\infty} d\xi'\, Y_w(\xi', t) \frac{\sin[C(\eta + \beta)]}{\cosh[C(\xi' - \xi)] - \cos[C(\eta + \beta)]}, \tag{26}$$

$$U_g = \frac{C}{2\pi} \int_{-\infty}^{+\infty} d\xi'\, Y_g(\xi', t) \frac{\sin[C(1 - \eta)]}{\cosh[C(\xi' - \xi)] - \cos[C(1 - \eta)]}, \tag{27}$$

The integrands in (26) and (27) have delta-function type singularities (at $\eta = -\beta$ for U_w, at $\eta = 1$ for U_g). These can be eliminated by partial integration before considering the η-differentiations of U_w and U_g which are necessary for the evaluation of the right-hand sides of Eqs. (17) and (18). From (26), for example, one gets

$$U_w = -\frac{1}{\pi} \int_{-\infty}^{+\infty} d\xi' \frac{\partial Y_w}{\partial \xi'} \arctan\left[\frac{\tanh[C(\xi' - \xi)/2]}{\tan[C(\eta + \beta)/2]}\right]. \tag{28}$$

To complete the determination of the mapping from (x, y) to (ξ, η), Eqs. (6) and (7), it is necessary to calculate X by (8). Straightforward calculations lead to

$$X(\xi, \eta, t) = \frac{C}{2\pi} \int_{-\infty}^{+\infty} d\xi' \frac{Y_w(\xi', \eta, t) \sinh[C(\xi - \xi')]}{\sinh^2[C(\xi - \xi')/2] + \sin^2[C(\eta + \beta)/2]} - \frac{C}{2\pi} \int_{-\infty}^{+\infty} d\xi' \frac{Y_g(\xi', \eta, t) \sinh[C(\xi - \xi')]}{\sinh^2[C(\xi - \xi')/2] + \sin^2[C(1 - \eta)/2]}. \tag{29}$$

5. The η-Coordinate of the Sink

It has been noted that the ξ-coordinate of the sink is zero but that the η-coordinate must be calculated at each value of time (see the remarks following (11)). The equation defining η_S is $y(0, \eta_S) = 0$, i.e., by (7), (24), (26), and (27),

$$\eta_S + \frac{C \sin \alpha_S}{2\pi} \int_{-\infty}^{+\infty} d\xi' \left[\frac{Y_w(\xi')}{\cosh C\xi' - \cos \alpha_S} + \frac{Y_g(\xi')}{\cosh C\xi' + \cos \alpha_S} \right] = 0, \tag{30}$$

where

$$\alpha_S = C(\eta_S + \beta). \tag{31}$$

When Y_w and Y_g are known, this equation can be solved by any of the standard methods, preferably by one which makes use of the fact that an approximate value of η_S is known at time t, namely the value calculated at an earlier time. Also,

$$\eta_S = 0 \qquad \text{at} \quad t = 0. \tag{32}$$

6. The Movement of the Boundaries

The movement of the boundaries is given by the solution to the initial-value problem defined by Eqs. (17)–(19). Equations (17) and (18) are nonlinear, coupled, integro-differential equations. In this section, critical time is defined and two methods of numerical solution are outlined.

6.1. *Definition of Critical Time*

Calculations break down when one or both denominators in (17) and (18) vanish, thus implying an infinite velocity of boundary displacement. This happens at a time called "critical time," t_c. Assuming that the boundaries are smooth at all times, except possibly at t_c, the vanishing of a denominator is seen to happen at $\xi = 0$, where (17) and (18) can be written

$$\left[\frac{\partial Y_f}{\partial t} \right]_{\xi = 0} = \frac{[\partial \phi / \partial \eta]_{\xi = 0, \eta = m}}{1 + [\partial Y / \partial \eta]_{\xi = 0, \eta = m}},$$

where $m = -\beta$ $(+1)$ if $f = w(g)$. Numerical evaluation actually shows that the denominator in the expression above is close to but less than one at small values of time and decreases to zero as time increases. When the velocity at that point of the boundary becomes infinite, one expects the appearance of a cusp and a discontinuous transition to a flow of quite a different type than the one assumed in the present model. (For infinite speeds at the boundary in similar problems see Ockendon in [5].) Calculations must be stopped at a time, less than t_c, when the denominator has become smaller than some positive number, say ε. Satisfactory approximations for t_c can be obtained by reducing the time step when the denominator becomes small and by choosing a small value for ε.

There is an interesting geometrical interpretation for the breakdown of the calculations at t_c. It can be shown that the denominators in (17) and (18) are the values at the boundaries of the function h^2 appearing in the expression for the infinitesimal length,

$$ds^2 = h^2(d\xi^2 + d\eta^2).$$

In other words, breakdown occurs when a concentration point appears in the (ξ, η) coordinates. In the case considered here two concentration points can appear simultaneously since the denominators in (17) and (18) can vanish at the same time.

6.2. *Solution for Small Q (Large Critical Times)*

The following method of solution is applicable to a large class of differential equations [9] but, as shown below, becomes unpractical for the solution of the problem at hand if the rate Q becomes larger than a certain value. In this method, Eqs. (17) and (18) are converted into an infinite set of coupled, ordinary, first-order differential equations by expanding Y_w and Y_g in Fourier series with time-dependent coefficients [9]. Thus it is first necessary to change the variable ξ, which has an infinite range, to a variable θ having a finite range. Among the likely $\xi(\theta)$ formulas, the following is implied by the hyperbolic cosine in (26) and (27):

$$\exp(C\xi) = \tan(\theta/2), \qquad 0 \leqslant \theta \leqslant \pi. \tag{33}$$

When (33) is used to obtain, say, $\partial Y/\partial\eta$ at $\eta = -\beta$ (see (17)), one gets

$$\left[\frac{\partial Y}{\partial \eta}\right]_{\eta = -\beta} = \frac{C}{2\pi} \sin\theta \int_0^{\pi} \frac{d\theta'}{\cos\theta - \cos\theta'} \left[(\sin\theta + \sin\theta')\, \partial Y_w/\partial\theta' \right.$$

$$\left. - (\sin\theta - \sin\theta')\, \partial Y_g/\partial\theta'\right], \tag{34}$$

where the Cauchy principal value must be taken and where use has been made of the symmetry of $Y_w(\theta)$ and $Y_g(\theta)$ around $\theta = \pi/2$ (implied by the symmetry of

$Y_w(\xi)$ and $Y_g(\xi)$ around $\xi = 0$. Similar formulas can be obtained for the other terms appearing in (17) and (18).

The Fourier transforms introduced now are

$$Y_w = \sum_{k=0}^{\infty} \frac{A_k(t)}{2k+1} \sin(2k+1)\,\theta, \qquad Y_g = -\sum_{k=0}^{\infty} \frac{B_k(t)}{2k+1} \sin(2k+1)\,\theta, \tag{35}$$

where the division by $2k+1$ is a matter of convenience and where the fact that only odd frequencies appear is due to the symmetry of the functions about $\theta = \pi/2$. Taking this symmetry into account and also the fact that $Y_w(\theta)$ and $Y_g(\theta)$ vanish at $\theta = 0$ and π (see (20)), sine series have been chosen so as to obtain the best possible convergence (see Ref. [11]). The trigonometric series in (35) thus represent periodic functions which are not only continuous but have, in addition, a first-order continuous derivative. This additional continuity would not have been observed by a cosine series.

Now using (35) in (34), inverting the order of integration and summation, and carrying out those integrals that can be found in the tables, one obtains

$$\left[\frac{\partial Y}{\partial \eta}\right]_{\eta=-\beta} = \frac{C}{2\pi} \sin\theta \sum_{k=0}^{\infty} [A_k c_k^-(\theta) - B_k c_k^+(\theta)], \tag{36}$$

where

$$c_k^{\pm} = \int_0^{\pi} \frac{\sin\theta' \cos(2k+1)\,\theta'}{\cos\theta - \cos\theta'}\, d\theta' \pm \pi \sin(2k+1)\,\theta. \tag{37}$$

Similar expressions can be obtained for the other terms appearing in (17) and (18). The right-hand sides of (17) and (18) are thus written as functions of θ and A_k and B_k, so that these equations can be written

$$\sum_{k=0}^{\infty} \frac{\dot{A}_k(t)}{2k+1} \sin(2k+1)\,\theta = F_A(\theta, A_1, A_2, ..., B_1, B_2, ...)$$

$$\sum_{k=0}^{\infty} \frac{\dot{B}_k(t)}{2k+1} \sin(2k+1)\,\theta = F_B(\theta, A_1, A_2, ..., B_1, B_2, ...),$$

where time derivatives on the left-hand sides are indicated by dots. Calculating the Fourier coefficients of the functions F_A and F_B, one obtains an infinite set of equations:

$$\dot{A}_k(t) = G_k(A_1, A_2, ..., B_1, B_2, ...), \qquad k = 1, 2, ... \tag{38a}$$

$$\dot{B}_k(t) = H_k(A_1, A_2, ..., B_1, B_2, ...), \qquad k = 1, 2, ... \tag{38b}$$

The calculation of the G_k and H_k is best done by using an algorithm for the fast Fourier transform (FFT) once a decision has been reached as to the maximum

number of equations (38) to be used. The techniques considered by Bellman and Adomian [9] for the choice of a maximum value of k are not easily applicable to the present case where calculations for small times show that A_k and B_k behave as $1/k$ for large k. We have adopted a method of closure which is more general than the ones considered in Ref. [9], based on acceleration of convergence [12, 13]. Briefly, acceleration consists in approximating the sum of an infinite series by a rational expression of a finite number of its first terms. This number is arbitrary and depends on the required accuracy. Very high accuracies can be obtained with few terms [12, 13], depending on how quickly the asymptotic behaviour of the kth term can be detected. Using acceleration of convergence on all the sums appearing in the problem, as in (35) and (36), it has been found that a maximum value of 8 for k is satisfactory as long as the rate Q is less than about 0.5. There are then 16 equations (38) to solve. These are in standard form and can be solved by any of the known methods, although stiff solvers turn out to give the best results. Note that the initial conditions attached to Eqs. (38) are, according to (19),

$$A_k(0) = B_k(0) = 0, \qquad k = 1, 2, \ldots .$$

It must be mentioned for completeness that η_S, which appears in (17) and (18) in the terms $\partial\phi/\partial\eta$ at $\eta = -\beta$ and 1, must be provided as a function of the A_k and B_k. This is done by using (33) and (35) in (30).

Knowledge of the vertical boundary displacements makes it then possible to calculate the horizontal boundary displacements (Eq. (29)), and the potential (Eq. (25)). Fast computational procedures are obtained if the sums in (35) are substituted in (25) and (29) and acceleration of convergence is used after inverting the order of integration and summation.

It has been mentioned that this solution is valid as long as Q is less than about 0.5. Above this rate, errors due to acceleration become large and the values of critical time start behaving erratically when plotted against Q. The reason for this is simply understood by referring to Fig. 2.

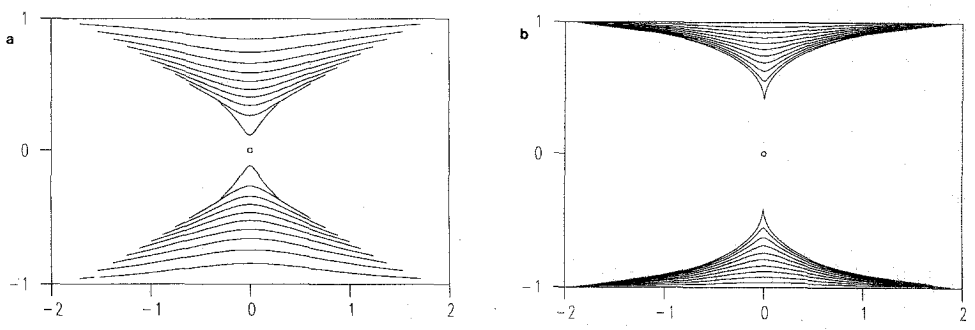

FIG. 2. Flow patterns for $\psi = \beta = 1$ and (a) $Q = 0.1$, (b) $Q = 1.0$. Critical times are 14.0 in (a) and 0.235 in (b). Boundaries are drawn at time intervals of $0.1t_c$.

Figure 2a shows the movement of the boundaries in the completely symmetric case $\psi = \beta = 1$ and for a rate $Q = 0.1$. Figure 2b corresponds to a rate of 1.0 (it has been produced with the second method, see Section 6.3). It can be seen (Fig. 2a) that the boundaries are relatively flat for the smallest rate, a peak developing inside a short time-interval just before critical time while, for the largest rate, the peak forms early in time (Fig. 2b). A sharp peak at a boundary implies that high frequencies become important in the Fourier expansions (35) so that, even using acceleration, one cannot avoid increasing the number of Eqs. (38) and computing-time becomes prohibitively large. One must then turn to the solution outlined below.

6.3. *Solution for Large Q (Small Critical Times)*

The second method for solving (17) and (18) is valid for large Q and is based on the observation that for large rates critical time becomes less than one. In this method the solution is taken to be the first iteration, given a zeroth approximation which is of a form suggested by the solution for $t \to 0$. Setting $t = 0$ in (17) and (18) and taking Eqs. (19) and (32) into account one obtains

$$\left[\frac{\partial Y_w}{\partial t}\right]_{t=0} = CQ \frac{\sin(C\beta)}{\cosh(C\xi) - \cos(C\beta)}, \tag{39}$$

$$\left[\frac{\partial Y_g}{\partial t}\right]_{t=0} = -CQ \frac{\sin(C\beta)}{\cosh(C\xi) + \cos(C\beta)}, \tag{40}$$

so that, for small times at least, Y_w and Y_g can be approximated by t times the right-hand side of, respectively, (39) and (40). We now assume a zeroth approximation of the form

$$Y_w(\xi, t) = CQ\gamma_w(t) \frac{\sin \alpha_S}{\cosh(C\xi) - \cos \alpha_S}, \tag{41}$$

$$Y_g(\xi, t) = -CQ\gamma_g(t) \frac{\sin \alpha_S}{\cosh(C\xi) + \cos \alpha_S}, \tag{42}$$

where γ_w and γ_g are two unknown functions of time and α_S is the parameter defined by Eqs. (30) and (31). When (41) and (42) are used in (26) and (27) one finds that the integrations can be performed by hand so that the right-hand sides of (17) and (18) can be expressed in terms of elementary functions of ξ, η_S, and γ_w and γ_g. Now using (41) and (42) in reverse so as to express the γ's in terms of the Y's, one arrives at

$$\dot{Y}_w(\xi, t) = H_w(\xi, \eta_S, Y_w, Y_g), \tag{43}$$

$$\dot{Y}_g(\xi, t) = H_g(\xi, \eta_S, Y_w, Y_g), \tag{44}$$

where time-differentiation is indicated by a dot. These equations can now be solved

by known methods for a given ξ. Note that Eq. (30) (where (41) and (42) are used, the integration done by hand, and the γ's expressed in terms of the Y's) must be taken into account so that η_S is an implicit function of ξ, Y_w, and Y_g.

When Y_w and Y_g are calculated for a selected array of ξ-values, one may then proceed with the calculation of the horizontal boundary displacements and of the potential by numerical integration of Eqs. (25) and (29). We have performed this integration by first fitting splines through the calculated values of Y_w and Y_g and then using known quadrature methods.

6.4. *Joining the Two Solutions*

The two methods give, with some qualifications, the same solution for $\psi = \beta = 1$ and Q in the range 0.4 to 0.5. The practical significance of the case $\psi = \beta = 1$ will be discussed in Section 7; it is sufficient for the present discussion to remember that, due to the symmetry, $Y_g = -Y_w$. Here we shall compare the methods for $\psi = \beta = 1$ and $Q = 0.45$.

Critical time is 0.7 when acceleration is used while the iteration method gives 0.74. (See also Fig. 4 where differences in critical time are shown for $0.4 \leqslant Q \leqslant 0.5$.) When, for a given t between 0 and 0.695, the curve $Y_w(\theta, t)$ versus θ, given by acceleration, is compared to the corresponding curve given by iteration one finds deviations which are roughly independent of θ but which increase with time, from 0 at $t = 0$ to about 4 % at $t = 0.695$. These deviations are shown in Fig. 3 for $\theta = \pi/2$.

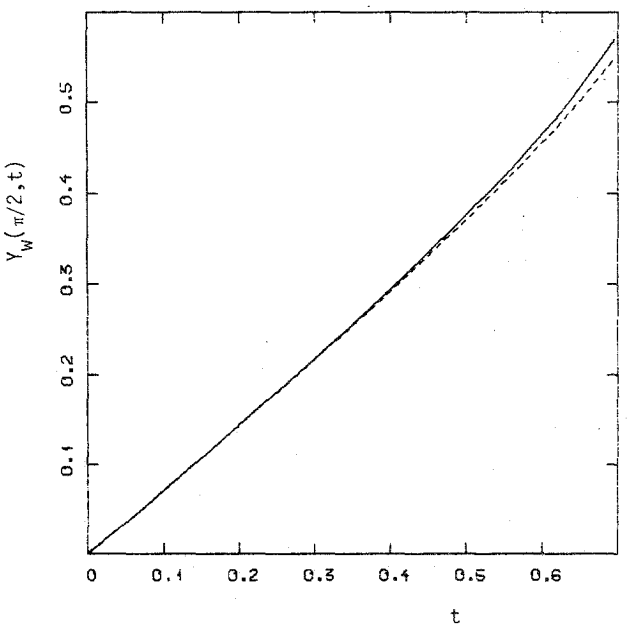

FIG. 3. $Y_w(\pi/2, t)$ vs t for $\psi = \beta = 1$ and $Q = 0.45$. The full line is obtained by acceleration, the

The full and broken lines show $Y_w(\pi/2, t)$ vs time for the accelerated solution and the iterated solution, respectively.

Assuming that, for all practical purposes, one can go from the acceleration method to the iteration method when the rate becomes larger than about 0.45, we now turn to the questions which were formulated in the Introduction.

7. Results and Conclusions

It is natural to look at critical time as a function of Q, ψ, and β:

$$t_c = t_c(Q, \psi, \beta).$$

The product Qt_c is the total amount of fluid removed, from time zero until t_c, and it is important to be able to predict the position of the well (in other words, the value of β) which gives the largest value of t_c for a given rate Q and given fluid properties (ψ). The full lines in Fig. 4 are the plot of t_c vs Q for $\psi = \beta = 1$, obtained by acceleration (line to the left) and iteration (line to the right). The particular significance of the function $t_c(Q, 1, 1)$ is to be found in the following properties of Eqs. (17) and (18). First,

$$t_c(Q, \psi, \beta) \leqslant t_c(Q, 1, 1). \tag{45}$$

Second, given Q and ψ (which is the usual situation), one can find one (and only one) value of β such that the equality in (45) holds. Finally, for such values of Q, ψ, and β, both boundaries develop a cusp at the critical time. We have not attempted to prove these statements mathematically, but have verified that they hold on a large number of cases, letting the parameters vary inside their likely physical ranges.

An example is shown by the broken line in Fig. 4 which is $t_c(Q, \frac{1}{2}, 1)$ vs Q. For all points on this curve the cusp appears at the lower boundary, as shown on Fig. 5a which correspond to point A ($Q = 0.3$, $\psi = 0.5$, $\beta = 1$) in Fig. 4. By increasing the value of β to 1.1 (point B, and corresponding flow pattern of Fig. 5b) one increases the critical time. The value $\beta = 1.333$ is the one that makes the equality in (45) hold. This gives point C in Fig. 4 and the corresponding flow pattern with a cusp at each boundary is shown in Fig. 5c. An increase of the value of β beyond the optimum (1.333) will then bring about a decrease in the critical time and a flow pattern where the cusp appears only at the upper boundary. The present example also shows that it is important to find the correct value of β as long as the rate Q is less than about 1. For larger rates the optimum value of β does not significantly increase t_c. This is confirmed by calculations with other values of ψ.

Since critical time increases as the rate decreases (Fig. 4), is it possible to find, for given ψ and β, a rate Q_s such that, for all $Q \leqslant Q_s$, the boundaries tend asymptotically to a static limit? We shall show that there is evidence against such a static limit by an argument based on perturbation theory. To simplify, we assume

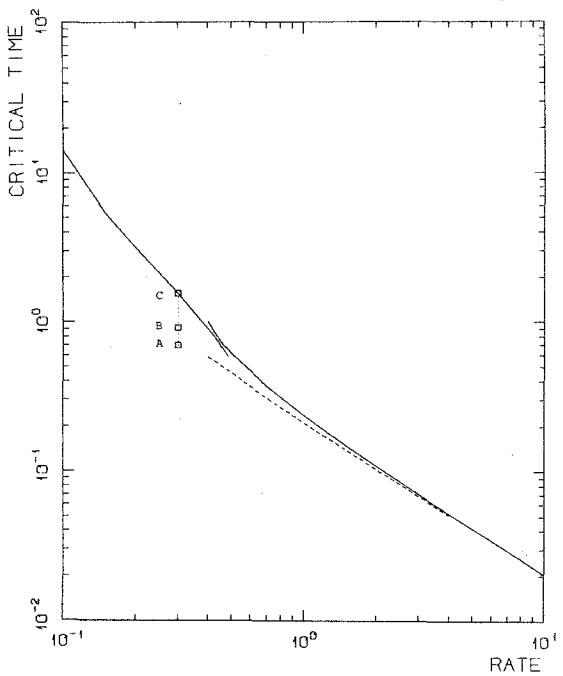

FIG. 4. Critical time vs rate: $\psi = \beta = 1$ for the full lines; $\psi = 0.5$, $\beta = 1$ for the broken line. At A: $\psi = 0.5$, $\beta = 1.0$; at B: $\psi = 0.5$, $\beta = 1.1$; at C: $\psi = 0.5$, $\beta = 1.333$.

$\psi = \beta = 1$, then look for a time-independent solution to Eq. (17), where the left-hand side is set equal to zero, in the form of an expansion,

$$Y_w(\theta) = \sum_{n=1}^{\infty} Q^n w_n(\theta).$$

The numerator on the right-hand side of (17) can then be written as an expansion in powers of Q. Equating all coefficients to zero one gets a recurrence scheme for the w_n. The equation for w_1 is

$$\frac{1}{\pi} \int_0^{\pi} d\theta' \frac{dw_1}{d\theta'} \frac{\sin \theta'}{\cos \theta - \cos \theta'} = -1,$$

where a principal value integration is implied. This equation has no solution because integration of the right-hand side between zero and π does not give zero [14]. There is a more general proof of the non-existence of a static limit to the present problem [15] but it is outside the scope of this paper.

In industrial applications the potential (which is related to the pressure by Eq. (A1) of the Appendix) is measured at the well and compared to theoretical predictions. In the model presented in Section 2 the sink is a point, which implies a

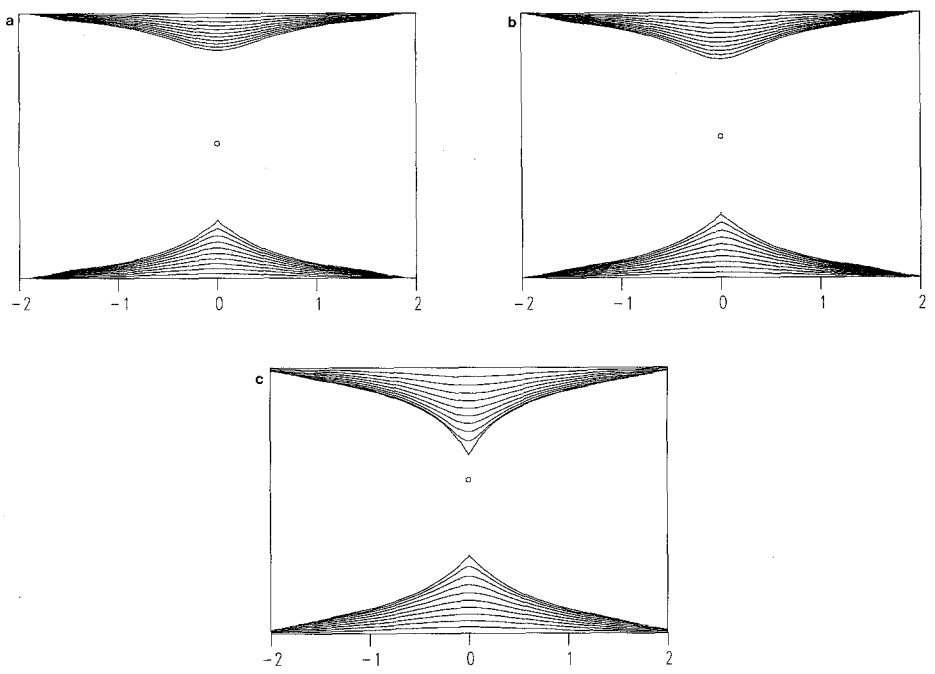

FIG. 5. Variation of flow pattern with sink position: $\psi = 0.5$ and $Q = 0.3$. In case (a) $\beta = 1$; case (b) $\beta = 1.1$, and case (c) $\beta = 1.333$. Figures a, b, and c correspond to points A, B, and C of Fig. 4, respectively. Boundaries are drawn at time intervals of $0.1t_c$.

well of zero radius and consequently an infinite potential at the well. This difficulty can be removed by calculating the potential at a small distance r_w from the sink, then subtracting the value of the potential at r_w and zero time. It can be shown that, because of the assumption of incompressibility (see Section 2), the potential which one thus subtracts is the value that the potential would take after infinite time if the boundaries were fixed and if compressibility was taken into account. This "renormalized" potential is shown in Fig. 6, plotted versus time for the case $\psi = \beta = 1$ and a range of Q-values. It is noteworthy that the potential can increase at the well for large rates.

In view of the high velocities attained by the boundaries near critical time, the question arises as to the validity of the present model since, as stated in Section 2, it is assumed that gas and water are in static equilibrium. This is equivalent to asking how high the velocities in these fluids can become before the assumption of static equilibrium breaks down. The question cannot be answered in general terms and must be considered in each case, together with information on the properties of the fluids in presence (densities, viscosities, relative permeabilities). In addition, one should consider the possibility of fingering-instability where a "finger" might develop as soon as a boundary has acquired a pronounced bulge. Such con-

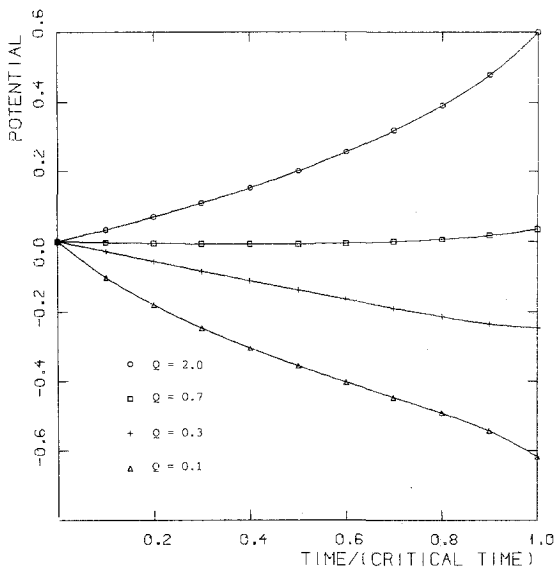

FIG. 6. Renormalized potential near the sink vs time for $\psi = \beta = 1$ and four different rates.

siderations fall outside the scope of this paper but it is probable that, at least for small rates ($Q \leqslant 0.4$), the model is realistic for a large range of fluid properties since the boundaries are then flat and move slowly until very shortly before critical time.

APPENDIX:
PHYSICAL QUANTITIES AND THEIR DIMENSIONLESS COUNTERPARTS

Only dimensionless quantities have been used in the main text and, as often as possible, without sub or superscripts. The relations between physical and dimensionless quantities are given below, where a star is added as a superscript to the symbols representing the physical coordinates and the physical time, rate, and potential. The corresponding symbols for the undimensional variables are left unstarred.

The nomenclature is as follows (SI units are indicated):

a = distance between sink and upper boundary at zero time (m)

b = distance between sink and lower boundary at zero time (m)

g = acceleration due to gravity ($m.s^{-2}$)

K = absolute permeability of the porous medium (m^2)

Q^* = rate of fluid withdrawal by unit length of well ($m^2.s^{-1}$)

p = pressure (Pa)

t^* = time (s)

$x^*, y^* =$ coordinates (m)

$\mu =$ oil viscosity (Pa.s)

$\rho =$ mass per unit volume;
always with an index g, o, or w (kg.m^{-3})

$\varphi =$ porosity.

The velocity potential is defined as

$$\phi^* = p + g\rho_0 y^* - p(x^* = \infty, y^* = 0). \tag{A1}$$

The relations between the physical quantities and their dimensionless counterparts used in the main text are

$$\phi = \frac{\phi^*}{ag(\rho_0 - \rho_g)},$$

$$t = \frac{Kg(\rho_0 - \rho_g)}{\mu a \varphi} t^*,$$

$$Q = \frac{\mu}{2\pi Kag(\rho_0 - \rho_g)} Q^*.$$

ACKNOWLEDGMENTS

We express our thanks to Steinar Ekrann and to Svein Skjaeveland for useful discussions about multiphase flow in porous media.

REFERENCES

1. M. MUSKAT, *Physical Principles of Oil Production* (International Human Resources Development Corporation, Boston, 1981), p. 226.
2. J. CRANK, *Free and Moving Boundary Problems* (Oxford Univ. Press (Clarendon), Oxford, 1984), p. 16.
3. S. RICHARDSON, *J. Fluid Mech.* **56**, 609 (1972).
4. A. A. LACEY, *J. Austral. Math. Soc. Ser. B* **24**, 171 (1982).
5. D. G. WILSON, A. D. SOLOMON, AND P. T. BOGGS (Eds.), *Moving Boundary Problems* (Academic Press, New York, 1978), p. 129.
6. J. M. AITCHISON AND S. D. HOWISON, *J. Comput. Phys.* **60**, 376 (1985).
7. R. V. CHURCHILL AND J. W. BROWN, *Complex Variables and Applications* (McGraw–Hill, Tokyo, 1984), 4th ed., p. 228.
8. G. RYSKIN AND L. G. LEAL, *J. Comput. Phys.* **50**, 71 (1983).
9. R. BELLMAN AND G. ADOMIAN, *Partial Differential Equations* (Reidel, Dordrecht, 1985), p. 153.
10. W. E. WILLIAMS, *Partial Differential Equations* (Oxford Univ. Press (Clarendon), Oxford, 1980), p. 125.
11. G. DAHLQUIST AND Å. BJORCK, *Numerical Methods* (Prentice–Hall, Englewood Cliffs, NJ, 1974), p. 417.
12. S. Å. GUSTAFSON, *Computing* **21**, 53 (1978).
13. S. Å. GUSTAFSON, *Computing* **21**, 87 (1978).
14. H. HOCHSTADT, *Integral Equations* (Wiley, New York, 1973), p. 160.
15. S. EKRANN, private communication.